Effect of graphite nanosheets on electrical, electromagnetic, mechanical and morphological characteristics of PHBV/GNS nanocomposites

Larissa S. Montagna[1*], Thaís L. do A. Montanheiro[1], Maurício R. Baldan[2], Ana Paula S. Oliveira[2], Marcelo A. de Farias[3], Marcele A. Hocevar[4], Luiza C. Folgueras[1,5], Fábio R. Passador[1], Ana Paula Lemes[1], Mirabel C. Rezende[1]

[1] *Institute of Science and Technology, Technology Laboratory of Polymers and Biopolymers (TecPBio), Federal University of São Paulo (UNIFESP), São José dos Campos, SP, Brazil*
[2] *Associated Laboratory of Sensors and Materials (LAS), National Institute for Space Research (INPE), São José dos Campos, SP, Brazil*
[3] *Brazilian Nanotechnology National Laboratory (LNNano/CNPEM), Campinas, SP, Brazil*
[4] *Laboratory of Polymeric Materials (LAPOL), Federal University of Rio Grande do Sul (UFRGS), Porto Alegre, RS, Brazil*
[5] *University of Taubaté (UNITAU), Mechanical Engineering Department, Taubaté, SP, Brazil*

*Corresponding author

DOI: 10.5185/amlett.2018.2044
www.vbripress.com/aml

Abstract

Bionanocomposites with properties similar to those of conventional polymers derived from petroleum have shown scientific and industrial interest. The current research discuss the effect of graphite nanosheets (GNS) addition on electrical, electromagnetic, and mechanical properties and also on morphological aspects of the natural polymer poly(hydroxybutyrate-*co*-hydroxyvalerate) (PHBV)/GNS nanocomposites and neat PHBV prepared by casting method. Nanocomposite of PHBV/1.00 wt% GNS showed good electrical conductivity values, extending the scope of application of these materials, such as in reflectors. One of the objectives of this study was to investigate the effect of different contents of GNS in neat PHBV using dynamic mechanical analysis (DMA), which showed that the addition of GNS in PHBV matrix improved the DMA properties. Transmission electron microscopy (TEM) shows good dispersion of GNS in the PHBV matrix with stacked and intercalated graphite layers and XPS confirmed the presence of carbon and oxygen in the graphite nanosheets surface.

Keywords: Poly(hydroxybutyrate-*co*-hydroxyvalerate), graphite nanosheets, nanocomposites, electrical conductivity, reflectivity.

Introduction

Natural, biodegradable, biocompatible and bioabsorbable polymers have received more attention recently by the researchers and industries because commercial polymers derived from petroleum are associated with environmental pollution. Thus, industrialists and scientific community are being encouraged by population in developing and applying clean technology in their products with raw materials derived from renewable sources, that will consequently reduce environmental impacts and contribute to sustainable development [1, 2].

One of the currently most widely used biopolymers is the poly(hydroxybutyrate-*co*-hydroxyvalerate) (PHBV), a copolymer from polyhydroxyalkanoates (PHAs) family, because these biopolymers have many advantages, besides being biodegradable and biocompatible have the processing capacity similar to conventional thermoplastics [3, 4]. However, these biopolymers present some disadvantages such as limited impact resistance due to high crystallinity, low performance of mechanical properties, electrical conductivity, thermal stability, hardness and also low melt viscosity [5]. Therefore nanoparticles, such as graphite nanosheets (GNS), are being incorporated into the PHBV matrix in order to improve these properties.

The choice of GNS is due to the fact that these nanoparticles are low-cost, abundant and show tremendous potential in improve mechanical, electrical and conductivity properties [6,7]. GNS based bionanocomposites, eco-friendly materials, have recently attracted significant interest at several applications, such as in electronics, aerospace and automotive devices, among other applications that are dominated by petroleum based materials [8, 9]. There are few studies related to bionanocomposites based on natural polymer reinforced with GNS, graphene nanosheets, graphene or graphene oxide [10,11, 12, 13, 14, 15]. All research papers mention the great

compatibility between the natural polymer and graphite, consequently the improvement of the properties analyzed.

In our previous work, we prepared PHBV/GNS nanocomposites at different GNS loadings (0.25, 0.50 and 1.00 wt% GNS), furthermore, we verified the effects of GNS on thermal and chemical properties of the PHBV/GNS nanocomposites [16]. The homogeneous dispersion of graphite nanosheets in PHBV matrix was one of the main objectives of the previous work, because of the high tendency of the nanoparticles to form aggregates and the preparation of PHBV/GNS nanocomposite has been performed in solution by solvent casting. Therefore, in the present work details of the morphology of nanocomposites by transmission electron microscopy (TEM) and the effects of GNS on electrical, electromagnetic and mechanical properties of PHBV/GNS nanocomposites are shown.

Experimental

Materials

Poly (hydroxybutyrate-*co*-hydroxyvalerate) (PHBV) with 4% of 3-hydroxyvalerate (HV) units and Mw 187,000 g.mol^{-1} was kindly supplied by PHB Industrial. The graphite used for the preparation of graphite nanosheets (GNS) was natural graphite flakes (NGF) from Sigma Aldrich (332461). Concentrated sulfuric and nitric acids from Chemical Company of Brazil (Vetec) were used as chemical intercalant and oxidizer to prepare the expanded graphite. The solvent used for the film preparation was chloroform ($CHCl_3$) (Vetec).

Method for Obtaining Graphite Nanosheets (GNS)

The methodology of obtaining the graphite nanosheets was already described by Montagna et al. [17]. Briefly, the process for preparing the graphite nanosheets is carried out in three steps: intercalation (chemical exfoliation), expansion (thermal treatment) and the graphite nanosheets obtainment (physical treatment by ultrasonic exfoliation).

Cast film preparation: Neat PHBV and PHBV/GNS nanocomposites

PHBV/GNS nanocomposites (0.25, 0.50 and 1.00 wt%) were prepared according to the methodology described by Montagna et al. [16] and Montanheiro et al. [18]. Initially, graphite nanosheets and chloroform (Vetec) (1:10 w/v) were sonicated for 4 h in an ultrasonic bath (Unique, USC1450). PHBV was solubilized in chloroform (1.1:10 wt/v) at 40 ºC. The system remained under magnetic stirring until all polymer mass has been dissolved and resulted in a viscous solution. Subsequently, the suspension containing the graphite nanosheets was stirred with PHBV solution for 3 h at 60 °C. The final solution was cast onto Petri dishes covered with aluminum foil to obtain films. Afterwards, the solvent evaporated at room temperature for 12 h.

Analytical characterization

The morphologies of graphite nanosheets and nanocomposites were characterized by transmission electron microscopy (TEM). Images of the graphite nanosheets were obtained using a 200 kV FEI Tecnai/G2 and the nanocomposites were acquired on a Jeol JEM-1400Plus (JEOL, Japan), operating at 120 kV with LaB_6 filament. PHBV/GNS nanocomposites were cut at -90°C, using a diamond knife, in a Leica EM FC6 cryo-ultramicrotome to supply ultrathin cross-sections (ca. 60 nm) for TEM observation. Thereafter, all the samples (GNS and nanocomposites) were prepared in Ultrathin carbon on a Lacey Carbon Type A 400 mesh copper grids (TedPella, USA).

The electrical conductivity of the GNS and the PHBV/GNS nanocomposites were measured using the four-point probe apparatus (Cascade Microtech CS4-64) associated to a Keithley 6430 Sourcemeter. Each value was based on a minimum of 3 measurement samples in the surface. The measurement of the samples in the form of film (0.023 mm) was performed at room temperature.

The electromagnetic characterization of PHBV/GNS nanocomposite was performed by reflectivity measurements of radiation incident on the material using the waveguide technique in the frequency range of 8.2 to 12.4 GHz (X-band) of the electromagnetic spectrum. The waveguide is coupled to a Microwave Network Analyzer from Agilent Technologies (PNA-L N5230C model) with 4 ports and frequency range 300 kHz to 20 GHz. An aluminum plate was used as reference material, i.e. 100% of reflection or 0% of attenuation, in the reflectivity measurements. The equipment was calibrated at 50 Ohms.

Dynamic mechanical analyses were performed using a TA Instruments Q800. Temperature range of -30ºC to 130ºC at a heating rate 3 ºC min^{-1} under nitrogen atmosphere, frequency of 1 Hz and 125% force track.

The chemical composition on sample surfaces was analyzed with an X-Ray photoelectron Spectroscopy Kratos Axis Ultra using a monochromated Al K_α X-ray source of 1486.68 eV. The survey XPS spectra were acquired with pass energy (PE) of 160 eV, 3eV step size, 200 ms dwell time and averaged over 3 scans. The high resolution C1s XPS spectra were acquired with PE of 40 eV, 0.1 eV step size, 100 ms dwell time and averaged over 5 scans. All the measurements were performed in ultra-high vacuum less than 10^{-7} Pa pressure, 15 kV acceleration voltages and 10 mA power emission. The XPS spectra were analyzed by fitting the data using a mixed Gauss-Lorentz product function after a Shirley type background subtracting. The peak fitting was performed using CasaXPS software and least-square fitting procedure was applied.

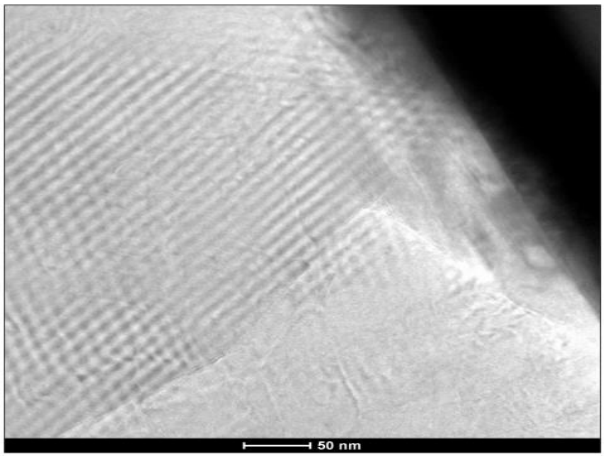

Fig. 1. TEM images of graphite nanosheets.

Results and discussion

Fig. 1 shows the micrographs with high magnification obtained by TEM of GNS, where it was possible to analyze the degree of exfoliation of the graphite sheets. The parallel lines, black-white, correspond to the various graphene sheets, which indicate the cross sections of the graphene sheets. The presence of these parallel lines may indicate that the crystalline structure of GNS is resistant to oxidation by strong acids (H2SO4/HNO3) and to expansion at elevated temperatures (~ 800 °C) [17].

Soin *et al.* [19] synthesized graphene by microwave plasma enhanced chemical vapors, deposition and obtained similar micrographs, in which the graphite flakes were indeed made up of large number of graphene layers.

Feng et al. [20] prepared graphene nanosheets on a large-scale via the deflagration of an obsoleted single base propellant in the presence of dibutyl phthalate (DBP) aiming to decrease the oxygen balance. Morphological analyses showed that the graphene nanosheets were shaped through the stacked graphene layer, of which the number could be estimated by the transparency of the graphene nanosheets, as the more transparent area means less stacked graphene layers.

According to Moniruzzaman and Winey [21], the dispersion and distribution of nanoparticles, like as graphene layers and GNS in the polymer matrix as well as their interfacial bonding are the two key factors of influence for the improvement of nanocomposite physical properties. Moreover, the dispersion method of nanoparticles in the polymer matrix is also a factor of extreme importance to obtain a homogeneous nanocomposite [22]. The used methodology for the GNS dispersing in chloroform at 60 ºC, followed by sonication during 4 h in an ultrasonic bath, was efficient to provide homogeneous nanocomposites. Therefore, **Fig. 2** shows TEM micrographs of the PHBV/GNS nanocomposites at loading of 1.00 wt% GNS. This image exhibits good dispersion of GNS in the polymer matrix with stacked and intercalated graphite layers. Graphite nanosheets dispersed in the PHBV matrix are delimited and highlighted with white circle and arrows in **Fig. 2**. Thus, it is observed that the dark lines present in the micrograph refer of GNS and are distributed in the matrix of PHBV (clear part of micrograph).

Barret *et al.* [15] prepared nanocomposite materials using thermally reduced graphene (TRG) in a renewable biopolymer, poly(hydroxyalkanoate) (PHA) matrix. These authors verified in TEM images of the composite with a loading of 0.5 wt% a good dispersion of graphene in the matrix, as indicated by the existence of transparent, likely single layer, graphite sheets.

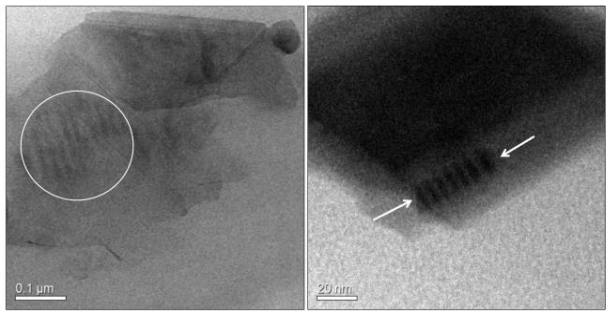

Fig. 2. TEM images of PHBV/GNS nanocomposites.

Wang and Qiu [12] investigated the influence of graphene oxide (GO) on biodegradable poly(l-lactic acid) (PLLA) by TEM, which indicated a relatively fine dispersion of GO in the PLLA matrix, meaning that GO has been mainly exfoliated and randomly dispersed on the molecular level.

In this work, the incorporation of GNS in PHBV matrix aimed to make nanocomposites of isolate matrix on a semiconductor. The PHBV/GNS nanocomposites may exhibit high electrical conductivity of about 10^{-4} S/cm at room temperature, as observed by Qiang Yin et al. [23] and V.S. Mironov et al. [24]. The high values presented by the nanocomposites were justified by the electrical conductivity of GNS, of 1.2 S/cm. Polymer materials have values of thirteen orders of magnitude lower, such as PHBV with 5.1 x 10^{-13} S/cm, value which was measured in a previous work [18].

The results of electrical conductivity indicated that the addition of higher content of GNS, 1.00 wt%, increased PHBV conductivity to 4.6 x 10^{-4} S/cm. Nanocomposites containing smaller GNS contents (0.25% and 0.50%) had immeasurable values of conductivity.

The increased conductivity of nanocomposites containing the highest GNS content (1.00 wt%) can be related to the good exfoliation of the graphite, obtained by chemical, physical and thermal methods, and the optimum dispersion of GNS in PHBV matrix, resulting in a greater number of dispersed particles per unit of area, creating more conductive points in the matrix, i.e., generating conducting networks in the sample [25]. The other samples (PHBV/0.25 wt% GNS and PHBV/0.50 wt% GNS) suggest did not have enough particles to promote electrical current conduction through the sample or the used equipment is not adequate for these measurements.

Several studies of electrical conductivity have been conducted in nanocomposites with derivatives of graphite in polymer matrices, and significant gains in the electrical conductivity of the final material are reported [26, 27]. There are no studies on literature related to the incorporation of GNS on biodegradable polymeric matrices, in order to obtain a semiconductor nanocomposite, only research related to the addition of carbon nanotubes in biodegradable matrices [18, 28].

Kalaitzidou et al. [26] studied the increase in conductivity of polypropylene, considered an insulating material, having electrical conductivity of about 10^{-18} S/cm, by coating the polymer with graphite nanoplatelets. The authors obtained final values of electrical conductivity for the nanocomposite in the order of 10^{-3} S/cm, and higher electrical conductivity value not found yet for this type of nanocomposite.

Ferreira [27] observed on a study obtaining polypropylene nanocomposites with exfoliated graphite that the addition of 12% of graphite in the polypropylene matrix made possible to obtain a material with semiconductive characteristics, i.e., conductivity on the order of 10^{-6} S/cm.

Electrical conductivity values achieved in this research for the nanocomposite PHBV/1.00% GNS extends the scope of application of these materials, such as in shielding for electromagnetic interference [9, 29]. Among the characteristics of a material used as electromagnetic shielding, is the good rate of absorption and reflection, both features can be obtained by incorporating ferromagnetic fillers, or naturally conductive particles [30, 31].

Fig. 3 shows the electromagnetic behavior by means of reflectivity curves in the frequency range of 8.2 – 12.4 GHz of nanocomposites PHBV/GNS with different contents of graphite nanosheets (0.25 wt%, 0.50 wt% and 1.00 wt% GNS) and thickness of 33 µm. It can be observed that all specimens present reflectivity values varying up to -1 dB (close to the reference aluminum plate). This behavior suggests an accentuated reflector behavior for the films studied, considering that all samples are conducting composites filled with GNS. As previously cited, the literature mentions several studies of electrical conductivity of polymeric nanocomposites with derivatives of graphite with significant values of electrical conductivity [26, 27].

Kashi *et al.* [11] studied biodegradable nanocomposites, and verified that the graphene nanoplatelet dispersed in natural polymer, polylactide (PLA), enhanced electromagnetic interference shielding performance.

Zhang *et al.* [32] prepared polymethylmethacrylate (PMMA) and GN samples with 2.0 mm-thickness by injection process, and obtained values of conductivity of 3.11 S/m and reflectivity of -19 dB, with the addition of 5 wt% graphene sheets. However, in the research of Youssef et al. [33] it was observed that the addition of 2wt% of graphene in epoxy matrix (specimen with 0.1mm - thickness) resulted in reflectivity values of -38 dB.

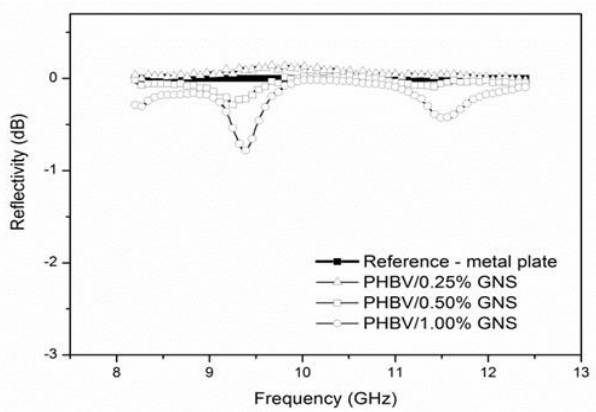

Fig. 3. Reflectivity curves *versus* frequency of the PHBV nanocomposites with 0.25, 0.50 and 1.00 wt% of GNS.

Lin *et al.* [34] prepared materials with 2.0 mm thickness based on water-based polyurethane with graphene oxide and silver nanoparticles. The electrical conductivity result obtained for nanocomposite with 5 wt% load was of 25.52 S/m and reflectivity values of -35 dB, in the frequency range 8.2-12.4 GHz (X-band).

Comparing the thickness of the samples prepared in the present work (33 µm) with those from literature (0.1 - 2.0 mm) [36, 37, 38] it is observed a marked difference. Considering that the thicknesses of samples have a significant influence on the microwave absorbing performance [35, 36], this comparison is impaired. However, the measured reflectivity results suggest that the studied films present a good performance as reflector material.

In order to investigate the improvement of mechanical behavior of PHBV with different contents of GNS (0.25, 0.50 and 1.00 wt%), mechanical testing by DMA was used to measure the storage modulus of PHBV samples. **Fig. 4** shows the effect of temperature on the storage moduli (E') of neat PHBV and PHBV/GNS nanocomposites. The analysis of these curves shows the their decreasing with the temperature increasing, with the most rapid reduction occurring from the glass transition region (T*g*) of PHBV, which is approximately 0.22 °C [18]. According to Chen et al. [37], the T*g* is related to the molecular motion, consequently affecting the molecular packing, chain rigidity and linearity.

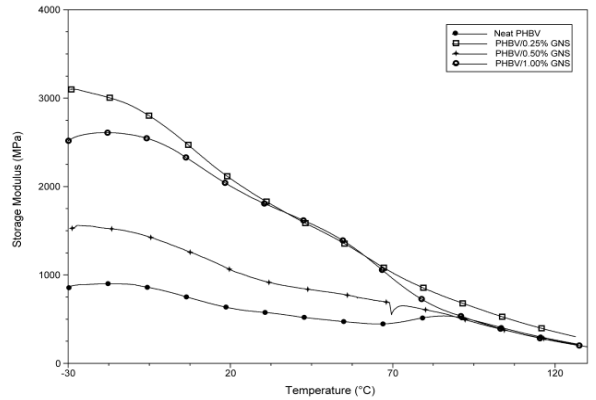

Fig. 4. Storage modulus (E') of the PHBV and PHBV/GNS nanocomposites as a function of temperature.

Thus, as the temperature increases, the polymers suffer the glass transition and the module undergoes a reduction in their value, because above the glass transition temperature the modulus of the sample significantly decreased due to the cooperative chain motion [38].

Storage moduli of PHBV matrix increase with the different content fraction of GNS, this increase is more evident in the sample containing the lowest content of GNS (0.25 wt% GNS) and followed by the highest GNS content (1.00 wt% GNS). The addition of different contents of GNS into PHBV matrix shows apparently to affect the viscoelastic behavior as considering variance of loss tangent in neat PHBV. Furthermore, according to Zhao et al. [39], the increase in storage modulus with the addition of nanoparticles in the polymer matrix can be attributed to the restriction of polymer chains.

The addition of GNS in the PHBV matrix induces a reinforcement effect, as observed for the values of E' at -30ºC that increased from around 800 MPa, for neat PHBV, to 3,200 MPa, 1,510 MPa and 2,500 MPa for PHBV/0.25% GNS, PHBV/0.50% GNS and PHBV/1.00% GNS, respectively. Therefore, the increase in the values of E' presented by the PHBV/GNS nanocomposites has been relatively significant when compared to neat PHBV, which may be attributed to the dispersion of GNS in the PHBV matrix (Fig. 2), indicating that GNS is an effective nanoparticle to enhance the dynamic mechanical properties of polymer.

In the study of Sridhar et al. [13], which verified the biodegradation of PHBV reinforced with graphenes and analyzed the dynamic mechanical properties, these authors observed the variation in storage modulus with temperature. In this study, the nanocomposites showed also higher modulus values than neat PHBV. This increase in the elastic modulus can be attributed to the immobilization of polymer chains onto the graphene surface, increasing the effective volume of the filler, these results were similar to those presented in the present research.

Srithep *et al.* [40] studied the influence of nanofibrillated (NFC) cellulose in PHBV matrix, and noted an increase of the storage modulus with the NFC content increasing, but the authors observed more significant increase in modulus above the glass transition temperature.

The survey XPS spectra were acquired to identify the elements present on the surface. The XPS spectra exhibited the characteristic peaks of GNS **(Fig. 5b)**. The XPS spectrum of GNS (C1s) is presented in **(Fig. 5a)**. The spectrum clearly indicates a considerable degree of oxidation with four components that correspond to carbon atoms in different functional groups. The signal at 284.8 eV exhibited the characteristic peaks of (C–C) while 286.7 eV indicates (C-O) groups. Besides, the peak at 286.9 eV was attributed to (C-OH/C-O-C/C-O-C=O), and the peak around 281.5 eV was assigned to (O-C(=O)-O).

The quantitative elemental composition on GNS revealed concentration of 98.73 % of carbon and 1.27 % of oxygen **(Fig. 5-b)** on the GNS surface. Similar results were observed in the study of Sridhar et al. [41] determined a concentration of 98.59 % of carbon and 1.41 % of oxygen on the graphene's surface.

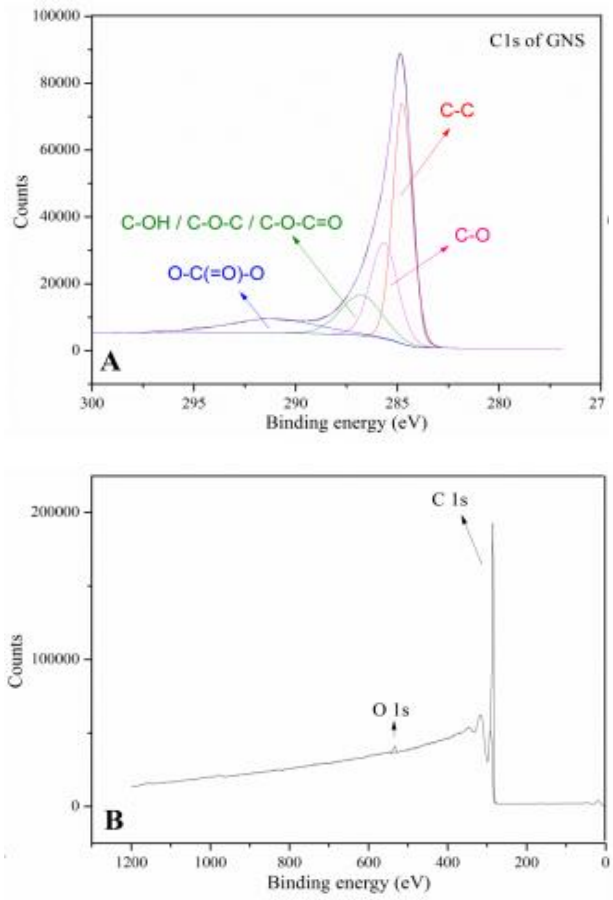

Fig. 5. XPS: (a) C 1s spectra of graphite nanosheets and (b) survey spectra of graphite nanosheets.

Conclusion

The morphology of PHBV/GNS nanocomposites analyzed by TEM showed good interaction and dispersion of GNS in the PHBV matrix, indicating that the methodology used to disperse GNS into PHBV matrix was efficient. GNS present high value of electrical conductivity, and when dispersed in PHBV matrix, turned an insulating matrix into a semiconductor nanocomposite. Reflectivity measurements in the frequency band of 8.2 -12.4 GHz suggest that the films studied presents reflector behavior due to the GNS filler contribution. DMA results suggest that the incorporation of GNS in PHBV matrix improved the thermal dynamic mechanical properties. XPS analysis was used for analyzed the surface chemistry of a material, that confirmed the presence of the carbon and oxygen on the graphite nanosheets surface.

Acknowledgements

The authors are grateful to CNPq (158961/2014-5 and 303287/2013-6), CAPES/PVNS and FAPESP (Brazil) for the financial supports. The authors would like to thank MSc. Eduardo Henrique Backes from DEMa/UFSCar for the dynamic mechanical analyses (DMA) and Eduardo do Valle Ricardo from Institute of Advanced Studies of the Sea of UNESP (*IEAMar*) by graphite nanosheets morphological analysis. The authors would also like to thank to LME/LNNano for the use of electron microscopy facility.

Author's contributions

The authors declare that there is no conflict of interest regarding the publication of this research paper.

References

1. Chang H.C.; Sun T.; Sultana N.; Lim M.M.; Khan T.H.; Ismail A.F. *Mater Sci Eng C Mater Biol Appl.*, **2016**, *61*, 396. **DOI**: 10.1016/j.msec.2015.12.074
2. Horny N.; Kanake Y.; Chirtoc M.; Tighzert L. *Polym Degrad Stab*., **2016,** *127*, 105. **DOI:** 10.1016/j.matchemphys.2017.03.036
3. Castro-Mayorga J.L.; Fabra M.J.; Pourrahimi A.M.; Olsson R.T.; Lagaron J.M. *Food and Bioprod Process*., **2017**, *101*, 32. **DOI:** 10.1016/j.fbp.2016.10.007
4. Dasan Y.K.; Bhat A.H.; Faiz A. *Carbohydr Polym*., **2017**, *157*, 1323. **DOI:** 10.1016/j.carbpol.2016.11.012
5. Ten E.; Jiang L.; Zhang J.; Wolcott M.P. *Biocomposites*, **2015**, 39. **DOI:** 10.1016/B978-1-78242-373-7.00008-1
6. Kyong H.; Kulkarni D.D.; Choi I.; Tsukruk V.V. *Prog Polym Sci*, **2014**, *39***,** 1934. **DOI:** 10.1016/j.progpolymsci.2014.03.001
7. Peponi L.; Puglia D.; Torre L.; Valentini L.; Kenny J. *Mater. Sci. Eng*., **2014**, *85*, 1. **DOI:** 10.1016/j.mser.2014.08.002
8. Mittal G.; Dhand V.; Rhee K.Y.; Park S.J.; Lee W.R. *J Ind Eng Chem*, **2015**, *21*, 11. **DOI:** 10.1016/j.jiec.2014.03.022
9. Gómes H.; Ram M.K.; Alvi F.; Villalba P.; Stefanakos E.; Kumar A. *J Power Sources*., **2011**, *196*, 4102. **DOI:** 10.1016/j.jpowsour.2010.11.002
10. Matilda, L.; Hetherington, C.J.D.; Wallenberg, R.; Jannasch, P. *Polym*., **2017**, *108***,** 66. **DOI:** 10.1016/j.polymer.2016.11.042
11. Kashi, S.; Cupta, R.K.; Baum, T.; Kao, K.; Bhattacharya, S.N. *Mater Des*, **2016**, *95*, 119. **DOI:** 10.1016/j.matdes.2016.01.086
12. Wang, H.; Qiu, Z. *Thermochim Acta*., **2011**, *526*, 229. **DOI:** 10.1016/j.tca.2011.10.006
13. Sridhar, V.; Lee, I.; Chum, H.H.; Park, H. *eXPRESS Polym Lett*., **2013**, *7*, 320. **DOI:** 10.3144/expresspolymlett.2013.29
14. Wang, B-j.; Zhang, U-j.; Zhang, J-q.; Gou, Q-t.; Wang, Z-b.; Chen, P.; Gu, Q. *Chin J Polym Sci*,. **2013**, *31*, 670. **DOI:** 10.1007/s10118-013-1248-1
15. Barrett, J.S.F.; Abdala, A.; Srienc, F. *Macromol*., **2014**, *47*, 3926. **DOI:** 10.1021/ma500022x
16. Montagna, L.S.; Montanheiro, T.L.A.; Machado, J.P.B.; Passador, F.R.; Lemes, A.P.; Rezende, M.C. *Intern J Polym Sci*., **2017**, *1*, 1. **DOI:** 10.1155/2017/9316761
17. Montagna, L.S.; Fim, F.C.; Galland, G.B.; Basso, N.R.S. *Macromol Symp*., **2011**, *299/200*, 48. **DOI:** 10.1002/masy.200900133
18. Montanheiro, T.L.A.; Cristóvan, F.H.;, Machado, J.P.B.; Tada, D.B.; Durán, N.; Lemes, A.P. *J Mat Res*., **2015**, *30*, 55. **DOI:** 10.1557/jmr.2014.303
19. Soin, N.; Roy, S.S.; O'Kane, C.; McLaughlin, A.D.; Lim, T.H.; Hetherington, C.J.D. *Cryst Eng Comm*., **2011**, 13, 312. **DOI:** 10.1039/C0CE00285B
20. Feng, W.; Chen, H.; Zheng, W.; Chen, Y.; Lin, X.; Pan, R. *Mater Lett*., **2017**, *190*, 131. **DOI:** 10.1016/j.matlet.2016.12.074
21. Moniruzzaman, M.; Winey, K. *Macromol*., **2006**, *39*, 5194. **DOI:** 10.1021/ma060733p
22. Lai, M.; Li, J.; Yang, J.; Liu, J.; Tong, X.; Cheng, H. *Polym Int.*, **2004**, *53*, 1479. **DOI:** 10.1002/pi.1566
23. Yin, Q.; Li, A-j.; Wang, W-q.; Xia, L-g.; Wang, Y-m. *J Power Sources*, **2007**, *165*, 717. **DOI:** 10.1016/j.jpowsour.2006.12.019
24. Mironov, V.S.; Kim, J.K.; Park, M.; Lim, S.; Cho, W.K. *Polym Test*., **2007**, *26*, 547. **DOI:** 10.1016/j.polymertesting.2007.02.003
25. Kim, H.; Miura, Y.; Macosko, C.W. *Chem Mat*., **2010**, *22*, 3441. **DOI:** 10.1021/cm100477v
26. Kalaitzidou, K.; Fukushima, H.; Drzal, L.T.A. *Compos Sci Technol*., **2007**, *67*, 2045. **DOI:** 10.1016/j.compscitech.2006.11.014
27. Ferreira CI 2012 PhD Thesis (Universidade Federal do Rio Grande do Sul).
28. Wu, D.; Lv, Q.; Feng, S.; Chen, J.; Chen, Y.; Qiu, Y.; Yao, X. *Carbon*, **2015**, *95*, 380. **DOI:** 10.1016/j.carbon.2015.08.062
29. Liang, J.J.; Wang, Y.; Huang, Y.; Ma, Y.F.; Liu, Z.F.; Cai, F.M.; Zhang, C.D.; Gao, H.J.; Chen, Y.S. *Carbon*, **2009**, *47*, 922. **DOI:** 10.1016/j.carbon.2008.12.038
30. Jiang, F.; Wang, X.; Wu, D. *Energy*., **2016**, *98*, 225. **DOI:** 10.1016/j.energy.2016.01.008
31. Dong, N.; Chen, L.; Yin, X.; Ma, X.; Sun, X.; Cheng, L.; Zhang, L. *Ceram Int*., **2016**, *42*, 9448. **DOI:** 10.1016/j.ceramint.2016.03.001
32. Zhang, H.; Yan, Q.; Zheng, W.; He, Z.; Yu, Z. *Appl Mater Interfaces*, **2011**, *3*, 918. **DOI:** 10.1021/am200021v
33. Yousefi, N.; Sun, X.; Lin, X.; Shen, X.; Jia, J.; Zhang, B. *Adv Mat*., **2014**, *26*, 5480. **DOI:** 10.1002/adma.201305293
34. Lin, S.C.; Ma, C.C.; Hsiao, S.T.; Wang, Y.S.; Yang, C.Y.; Liao, W.H.; Li, S.M.; Wang, J.A.; Cheng, T.Y.; Lin, W.C.; Yang, R.B. *Appl Surf Sci*., **2016**, *385*, 436. **DOI:** 10.1016/j.apsusc.2016.05.063
35. Pinto, S.S.; Rezende, M.C. *J Nanomater*, **2017**. ID 198978 **DOI:** 10.1155/2017/1989785
36. Pinto, S.S.; Rezende, M.C. *J Electron Mat*., **2017**, *46*, 4939. **DOI:** 10.1007/s11664-017-5492-y
37. Chen, G.X.; Hao, G.J.; Guo, T.Y.; Song, M.D.; Zhang, B.H. *J Mat Sci Lett*., **2002**, *21*, 1587. **DOI:** 10.1023/A:1020309330371
38. Ten, E.; Turtle, J.; Bahr, D.; Jiang, L.; Wolcott, M. *Polym.*, **2010**, *51*, 2652. **DOI:** 10.1016/j.polymer.2010.04.007
39. Zhao, H.; Cui, Z.; Wang, X.; Turng, L.S.; Peng, X. *Compos Part B*, **2013**, *51*, 79. **DOI:** 10.1016/j.compositesb.2013.02.034
40. Srithep, Y.; Ellingham, T.;Peng, Y.; Sabo, R.; Clemons, C.; Turng, L.S.; Pilla, S. *Polym Degrad Stab*, **2013**, *98*, 1439. **DOI:** 10.1016/j.polymdegradstab.2013.05.006
41. Sridhar, V.; Jeon, J.H.; Oh, I.K. *Carbon*., **2010**, *48*, 2953. **DOI:** 10.1016/j.carbon.2010.04.034

